Quantum phases of hardcore bosons in two coupled chains: A density matrix renormalization group study

Bradraj Pandey,[1] S. Sinha,[2] and Swapan K. Pati[1,3]

[1]*Theoretical Sciences Unit, Jawaharlal Nehru Centre for Advanced Scientific Research, Jakkur Campus, Bangalore 560064, India*

[2]*Indian Institute of Science Education and Research-Kolkata, Mohanpur, Nadia 741252, India*

[3]*New Chemistry Unit, Jawaharlal Nehru Centre for Advanced Scientific Research, Jakkur Campus, Bangalore 560064, India*

(Received 4 June 2014; revised manuscript received 12 May 2015; published 26 June 2015)

We consider hardcore bosons in two coupled chains of one dimensional lattices at half filling with repulsive intrachain interaction and interchain attraction. This can be mapped onto a coupled chain of spin-1/2 XXZ model with interchain ferromagnetic coupling. We investigate various phases of hardcore bosons (and related spin model) at zero temperature by a density matrix renormalization group method. Apart from the usual superfluid and density wave phases, pairing of interchain bosons leads to the formation of phases like pair superfluid and density wave of strongly bound pairs. We discuss the possible experimental realization of such correlated phases in the context of cold dipolar gas.

DOI: 10.1103/PhysRevB.91.214432 PACS number(s): 75.10.Pq, 05.10.Cc, 05.30.Jp

I. INTRODUCTION

After successful experimental realization of dipolar Bose-Einstein condensation (BEC) of ^{52}Cr [1], ^{164}Dy [2], and Rydberg atoms [3], the possibility of finding exotic phases like superfluid, pair-superfluid, supersolid, pair-supersolid, charge density wave, and phases involving quantum magnetism [4] have increased tremendously. Usually, bosons can form superfluid by condensation of bosonic particles to a single ground state, whereas fermionic superfluidity in superconductors and in cold atoms [5,6] occurs due to the formation of pairs. For sufficiently strong attractive interactions, bosons can also form pairs, which leads to the formation of "pair superfluidity" of bosons [7]. Pair superfluidity can be realized in cold atom systems by interspecies attractive interactions [8,9], bilayer dipolar systems [10–12], and through Feshbach resonance [13]. Theoretically, "pair superfluidity" has also been studied in models with correlated hopping [14].

A supersolid phase is described by simultaneous existence of crystalline order and superfluid order in the system. Various experimental and theoretical studies have been carried out for finding supersolidity [15–25]. Interestingly, pair supersolid (PSS) is defined as a phase where one finds simultaneous existence of pair superfluidity and modulation in density, with vanishing single-particle superfluidity [9–11,26]. Bilayer dipolar systems provide existence of pair-superfluid (PSF) and pair-supersolid (PSS) phases [10,11]. The possibility of pair supersolidity in bilayer dipolar gas with polarized dipoles has been also investigated [10], where the existence of PSF and PSS phases are shown by solving an effective Hamiltonian of pairs in the strong coupling limit.

Trefzger *et al.* have looked at polarized dipolar particles in two decoupled 2D layers, in the presence of repulsive interactions in the planes and attractive interactions between the two layers. They have shown the existence of PSS and PSF phases by solving the effective extended Bose-Hubbard Hamiltonian in the low-energy subspace of pairs, by means of a mean-field Gutzwiller approach and exact diagonalization methods [10]. The PSF and PSS phases have also been studied in a two-species Bose-Hubbard model in a two-dimensional square lattice with on-site intraspecies repulsions and interspecies attractions [9].

Low-dimensional quantum systems are quite unique, as in reduced dimension, quantum fluctuations destroy the true long range order (LRO). Instead, the low-dimensional systems quite often show quasi-long range order (QLRO). Incidentally, for the system to show QLRO, the equal-time correlation functions, $\langle C^{+}(X)C(0)\rangle$ (where X is the distance), would decay algebraically. However, if the correlation function decays exponentially, the system is believed to show short range order (SRO) [27]. The transition between superfluid to Mott insulator in one dimension at commensurate density is a BKT type transition, and the transition point can be determined by a Luttinger liquid parameter, K [28–33]. The Luttinger liquid parameter can be extracted from exponent of correlation functions. For bosonic low-dimensional systems, there have been studies where a number of phases, namely, superfluid, supersolid, and pair-superfluid phases, have been reported [34–46]. In low dimension, quite a few interesting studies in pairing phenomena have been carried out. Paired superfluid and counterflow superfluidity in one dimension can exist in a binary mixture of bosons with equal density [35]. Studies on phases of the dipolar bosonic gases in unconnected neighboring one-dimensional systems have also been carried out [34]. Parallel stack of one-dimensional hardcore bosons in optical lattices have been studied, by using bosonization and quantum Monte Carlo methods [45], where superfluids, supercounterfluids (SCF), and checkerboard (CB) phases from composite particles from different tubes are shown. In a recent study [46] of a two-leg ladder system with attractive on-site and repulsive interchain nearest-neighbor interactions, phases like atomic superfluid, dimer superfluid, and dimer rung insulator are found by imposing the on-site three-body constraint.

Motivated by recent experimental progress on dipolar gas, we consider hardcore bosons with dipolar interactions on two coupled one-dimensional chains at half-filling. Dipoles are oriented in such a way that it generates a nearest-neighbor intrachain repulsion and on-site interchain attraction. In this system, inter-chain attraction can induce pairing between the bosons in two chains and intrachain repulsion can break the translational symmetry which leads to the formation of density ordering. In this work, we mainly focus on the formation of various phases due to the interplay between these two

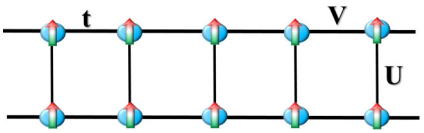

FIG. 1. (Color online) Schematic of the two chains with dipolar bosons. There is nearest-neighbor repulsive interaction V, and nearest-neighbor hopping parameter t, in each of the chains. Both chains are coupled with on-site attractive interaction U, while there is no hopping between the two chains.

orderings. The remaining part of the paper is organized as follows. In Sec. II we describe the model and its connection to an equivalent spin model. Various phases of this bosonic ladder (and spin chain) with different ordering are discussed. The results obtained from DMRG calculations are presented in detail in Sec. III. Different phases and their transitions are described in separate subsections. Finally, we summarize all our results in Sec. IV.

II. MODEL

We consider hardcore bosons in two coupled chains of one-dimensional lattices at half filling with dipolar interaction as depicted in Fig. 1. The anisotropic part of dipolar interaction is proportional to $(1-3\cos^2(\theta))$, where θ is the angle between the dipoles. We consider that the dipoles are polarized perpendicular to the chains (as shown in Fig. 1). Thus the dipolar interaction is repulsive when dipoles are in the same chain, while the dipoles of different chains which are at the same lattice site attract each other. The effective Hamiltonian of the system, without taking into account the interchain hopping, can be written as

$$H = -t\sum_{\alpha,\langle i,j\rangle}(b^{\dagger}_{\alpha,i}b_{\alpha,j}+\text{H.c.}) + V\sum_{\alpha,\langle i,j\rangle}\hat{n}_{\alpha,i}\hat{n}_{\alpha,j} - U\sum_{i}\hat{n}_{1,i}\hat{n}_{2,i}, \quad (1)$$

where $\alpha = 1,2$ is the chain index, t is the hopping term within the chains, V is the strength of intrachain nearest-neighbor repulsion, and U is the strength of interchain on-site attraction. For simplicity, we truncate the long range dipolar interaction and consider only nearest-neighbor intrachain repulsion and on-site interchain attraction. The physical states of a hardcore boson are restricted by the condition $b_i^{\dagger 2}|0\rangle = 0$. The number states of a hardcore boson are equivalent to s^z states of a spin-1/2 particle by the mapping ($|1\rangle \rightarrow |\uparrow\rangle$ and $|0\rangle \rightarrow |\downarrow\rangle$). The creation, annihilation operators of a hardcore boson can be represented by the spin-1/2 operators as follows: $s_i^+ \rightarrow b_i^{\dagger}$, $s_i^- \rightarrow b_i$, and $s_i^z \rightarrow n_i - 1/2$. The final spin Hamiltonian turns out to be a coupled chain of spin-1/2 XXZ model with interchain ferromagnetic coupling,

$$H = -t\sum_{\alpha,\langle i,j\rangle}(s^+_{\alpha,i}s^-_{\alpha,j}+\text{H.c.}) + V\sum_{\alpha,\langle i,j\rangle}s^z_{\alpha,i}s^z_{\alpha,j} - U\sum_{i}s^z_{1,i}s^z_{2,i}. \quad (2)$$

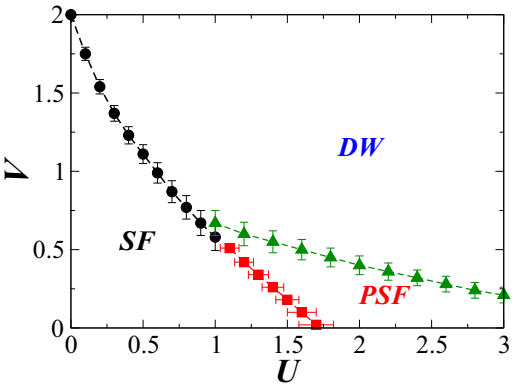

FIG. 2. (Color online) Two-dimensional phase diagram in the phase space of two parameters, U and V. The phase diagram is quite rich with phases, namely, superfluid (SF), pair-superfluid (PSF), and density wave (DW) phases.

In the spin Hamiltonian Eq. (2), which is obtained from the bosonic Hamiltonian [Eq. (1)], we impose the constraint $\sum_i s^z_{\alpha,i} = 0$.

In this model, we scale all the energies by the hopping strength, t, and set $t = 1$ to obtain the complete phase diagram in the $U - V$ plane. For $U = 0$, the above model becomes equivalent to two decoupled XXZ spin-1/2 chains which can be solved exactly and studied extensively [27]. This model undergoes a quantum phase transition to antiferromagnetic phase above the critical coupling value, $V = 2$. Similarly, hardcore bosons with nearest-neighbor repulsion exhibits a transition from superfluid to density wave. Superfluid and density wave phases can be characterized by following correlation functions,

$$C_{\alpha}(r) = \langle b^{\dagger}_{\alpha,i}b_{\alpha,i+r}\rangle, \quad (3)$$

$$G_{\alpha}(r) = \langle n_{\alpha,i}n_{\alpha,i+r}\rangle. \quad (4)$$

For spin chain, corresponding correlations functions transform to $C_{\alpha}(r) = \langle s^+_{\alpha,i}s^-_{\alpha,i+r}\rangle$ and $G_{\alpha}(r) = \langle s^z_{\alpha,i}s^z_{\alpha,i+r}\rangle$. In SF phase of bosons the correlation function $C_{\alpha}(r)$ shows power law decay $\sim 1/r^{\alpha_s}$, where the exponent α_s can be determined from the Luttinger parameter [27].

We have calculated relevant quantities by varying the values of the parameters U, V and the phase diagram is shown in Fig. 2. For low values of U and V, bosons in the two chains are almost decoupled and form a superfluid in each of the chains. In terms of spins, there will be quasi-long range order in the X-Y plane [21]. In this case, the effect of fluctuation is quite large and there is no order along the z axis. For sufficiently large nearest-neighbor interaction, density ordering develops in each chain which can be characterized by the density-density correlation function $(-1)^r G_{\alpha}(r)$. In DW phase, superfluidity vanishes and $C_{\alpha}(r)$ decays exponentially due to the appearance of an energy gap. Attractive interaction between two chains induces pairing of bosons which can be analyzed from the correlation function of the pairs,

$$P(r) = \langle b^{\dagger}_{1,i}b^{\dagger}_{2,i}b_{2,i+r}b_{1,i+r}\rangle - \langle b^{\dagger}_{1,i}b_{1,i+r}\rangle\langle b^{\dagger}_{2,i}b_{2,i+r}\rangle. \quad (5)$$

For sufficiently large attractive interaction, U, and small repulsive interaction, V, a quasi-"pair-superfluid" (PSF) state of bound pairs is formed. In this phase the correlation function, $P(r)$, shows QLRO but single particle superfluidity vanishes. In the large U and V limit, the system forms strongly bound pairs of hardcore bosons with density ordering of the pairs due to the strong nearest-neighbor repulsion. This insulating density wave phase of pairs can be described by the wave function,

$$|PDW\rangle = \prod_i |0,0\rangle_i \prod_j |1,1\rangle_j, \tag{6}$$

where i,j represent sites of two sublattices and $|n_1,n_2\rangle_i$ is the number state of coupled chains at site i. In terms of spin language, spins are ordered antiferromagnetically in each of the chains, while spins align ferromagnetically along the rung of the ladder. This phase is similar to the "pseudogap" phase of superconductors, where phase coherence between the strongly bound pairs is absent.

III. RESULTS AND DISCUSSION

To solve the above spin Hamiltonian and to find various possible quantum phases in the parameter space, we have used density-matrix renormalization group (DMRG) [47,48] method. We consider spin-1/2 at every site, varying the DMRG cutoff (max = m) from 250 to 400, for consistent results. Unless otherwise stated, most of the results below are obtained with $m = 250$. We have used an open boundary condition for both the chains. We have compared our DMRG results, namely energy gap and energy eigenvalues, with results from exact diagonalization, up to 28 lattice sites. We find the energies are comparable up to five decimal places. To characterize different phases, we have calculated spin density, two points and four points correlation functions, and the corresponding structure factors. For showing plots of correlation functions and structure factor, unless stated explicitly, we have considered each chain to be of length $L/2 = 160$, which amounts to the total system size $L = 320$. To determine an accurate phase boundary between different phases and to minimize the finite size effect, we have done finite-size scaling of correlation lengths, structure factors, and exponents of the correlation functions of the system with size (L) up to 384.

A. SF to DW transition

The quasisuperfluid order in terms of spin language can be described as order in the XY plane [21]. To calculate order along the XY plane, we have calculated transverse spin-spin correlation function $C_\alpha(r) = \langle S^+_{\alpha,0} S^-_{\alpha,r}\rangle$, where r is the distance from the middle of the chain. In Fig. 3, we have shown the plot of the correlation function, $C_1(r)$, at $U = 0.5$ and different values of V. It shows correlation function, $C_1(r)$, decays algebraically for $V = 0.4$ and 1.0, while it has short range order for $V = 1.4$. The structure factor $C_1(k) = \frac{1}{(L/4)} \sum \exp(ikr) C_1(r)$ gives peak at $k = 0$ in the superfluid phase. For characterizing order along the z axis (density wave), we have calculated the correlation function $G_\alpha(r) = \langle S^z_{\alpha,0} S^z_{\alpha,r}\rangle$. In Fig. 4, we have shown the plot of

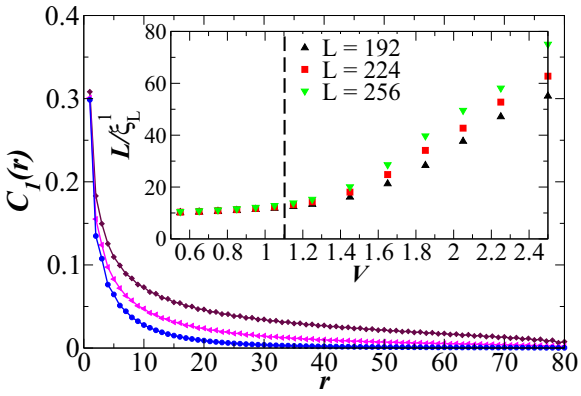

FIG. 3. (Color online) Plot of correlation function $C_1(r)$, as a function of r, at $U = 0.5$ and different values of V [$V = 0.4$ (square), $V = 1.0$ (triangle), and $V = 1.4$ (circle)]. Inset shows scaling of L/ξ_L^1 as a function of V for $U = 0.5$. Coalescence of the data points of different L shows SF-DW transition at $V = 1.1 \pm 0.05$.

correlation function, $(-1)^r G_1(r)$, at $U = 0.5$ and different values of V. The system has order along the z axis for $V = 1.2$ and 1.4, while it has short range order for $V = 0.4$. Due to the open-boundary condition in DMRG, there exists some fluctuations in $G_1(r)$ close to the boundary. The structure factor $G_1(k) = \frac{1}{(L/4)} \sum \exp(ikr) G_1(r)$ gives peak at $k = \pi$ in the density wave phase.

The transition between superfluid to gapped density wave in one dimension is a BKT type transition. Thus the system opens up a gap very slowly, as it makes the transition from SF to DW [28–30]. As energy gap and correlation length are related to each other ($G_L \sim 1/\xi_L$), superfluid to density wave transition can be shown by finite-size scaling of the correlation length. The correlation length is defined as [30,33,49,50]

$$\xi_L^\alpha = \sqrt{\frac{\sum_r r^2 C_\alpha(r)}{\sum_r C_\alpha(r)}}, \tag{7}$$

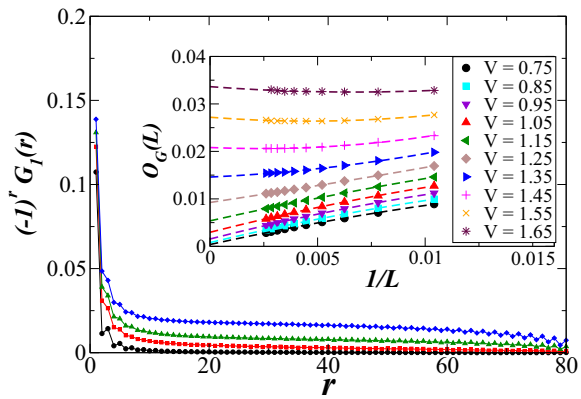

FIG. 4. (Color online) Plot of correlation function $(-1)^r G_1(r)$, as a function of r, at $U = 0.5$ and different values of V [$V = 0.4$ (circle), $V = 1.0$ (square), $V = 1.2$ (triangle), and $V = 1.4$ (diamond)]. Inset shows finite-size scaling of $O_G(L)$, at $U = 0.5$, and for different values of V.

where $C_\alpha(r) = \langle S^+_{\alpha,0} S^-_{\alpha,r} \rangle$ is obtained by using the wave function of the system of length L. In the inset of Fig. 3, we have plotted length dividing correlation length L/ξ^1_L versus V, for $U = 0.5$. The coalescence of data occurs at $V = 1.1 \pm 0.05$ for different system sizes ($L = 192,224,256$). This indicates a transition from SF to DW at $V = 1.1 \pm 0.05$.

Density wave order can also be characterized by a nonzero static structure factor, $O_G(L) = G_1(k = \pi) = \frac{1}{(L/4)} \sum_r (-1)^r G(r)$ [11,38,51,52]. To obtain the thermodynamic value of $O_G(L)$, we have done finite-size scaling for systems with length L up to 384, by fitting the finite-size $O_G(L)$ [38] values with a function, $O_G + O_1/L + O_2/L^2$. In the inset of Fig. 4, we have plotted $O_G(L)$ as a function of 1/L at $U = 0.5$ and different values of V. From inset of the Fig. 4, its appears that the extrapolated value of $O_G(L)$ is finite for $V \gtrsim 1.05$. On the contrary, for lower values of V, $O_G(L)$ decreases faster to very small values with an increase in system size. This should have gone to zero in the thermodynamic limit; however, due to the BKT nature of the transition, the extraploated value of $O_G(L)$ goes to small nonzero values, particularly near the critical region of SF-DW transition. In fact, due to the slow nature of the transition, from extrapolation of $O_G(L)$, it is difficult to exactly locate the phase boundary of the SF-DW transition. However, the significance of the $O_G(L)$ plot is that it shows how the DW wave appears in the system, while going from a SF to DW phase. Note that, in the density wave phase, $G_1(r)$ decays exponentially to a nonzero value (except for some fluctuations near the boundary). Therefore, as shown in Fig. 4, from correlation function $(-1)^r G_1(r)$ and finite-size scaling of O_G, we have estimated the density wave order in the system for $V = 1.1 \pm 0.08$, at $U = 0.5$.

As mentioned above, transition between SF to DW in one dimension is BKT type. The transition point can also be determined by examining the critical exponent of the correlation function [28,29,33]. Critical exponent can be obtained by fitting the correlation function with algebraic decay of $C_1(r) = A/r^{2K_C}$ [as shown in Fig. 5(c)]. At the transition point (from SF to DW), exponent (K_C) of the function $C_1(r)$ takes the value 1/2. The thermodynamic limit of $K_C(L)$ is obtained by extrapolating $K_C(L) = K_C + K_1/L + K_2/L^2$, where K_1 and K_2 are constants. In Fig. 5, we have shown SF to DW transition from K_C of the correlation function $C_1(r)$ at $U = 0.5$ and by varying V. In Fig. 5(a), we have shown extrapolation of $K_C(L)$, obtained from a power law fit of $C_1(r)$ for different system sizes. Extrapolation of $K_C(L)$ goes to 1/2 at $V = 1.12$ [inset of Fig. 5(b)]. This indicates a phase transition from SF to DW at $V = 1.12 \pm 0.04$ for $U = 0.5$. The error of ± 0.04 is the error in fitting of $C_1(r)$ to the algebraic function. In Fig. 5(c), we have shown fitting of a correlation function, with $C_1(r) = A/r^{2K_C}$ for $V = 1.0$, and with chain length $l = 128$. Due to the open boundary condition, fitting is not good near the end of the chain. Also while going from a SF phase to a DW phase, fitting error increases. For $U = 0$ and $V = 2.0$, which is the transition point from SF to DW, we find $K_C = 1/2 \pm 0.01$, while with increase in U near the SF-DW boundary, the error in fitting of $C_1(r)$ also increases slowly. The transition points obtained from scaling of the L/ξ^1_L and exponent $K_C(L)$ are consistent with each other within the error bars indicated in the phase diagram.

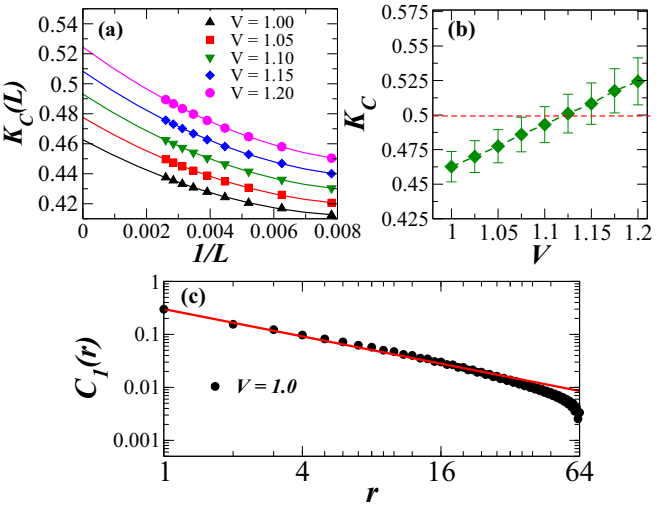

FIG. 5. (Color online) (a) Finite-size scaling of $K_C(L)$, at $U = 0.5$ and different values of V. (b) Plot of the extrapolated values of $K_C(L)$ vs V for $U = 0.5$, showing SF to DW transition at $V = 1.12 \pm 0.04$. (c) Power law fitting of $C_1(r)$ for $V = 1.0$, on a log-log scale.

B. SF to PSF transition

With increase in attractive interaction U along the rungs of the ladder, hardcore bosons start making pairs along these rungs. As a result, single particle superfluidity starts decreasing in each of the chains. For smaller values of repulsive interaction V, and sufficiently large values of U, the system shows BKT type transition from single particle superfluid phase to pair-superfluid phase [35,53]. In the PSF phase, single-particle spectrum opens up a gap. As a result, the correlation function, $C_1(r)$, decays exponentially in this phase. As discussed in the case of SF to DW transition, here also we estimate the SF to PSF transition from finite-size scaling of correlation length ξ^α_L. In Fig. 6, we have plotted $C_1(r)$ vs r at $V = 0.1$ and different values of U. This plot shows the transition from algebraic to exponential decay of $C_1(r)$, as the system

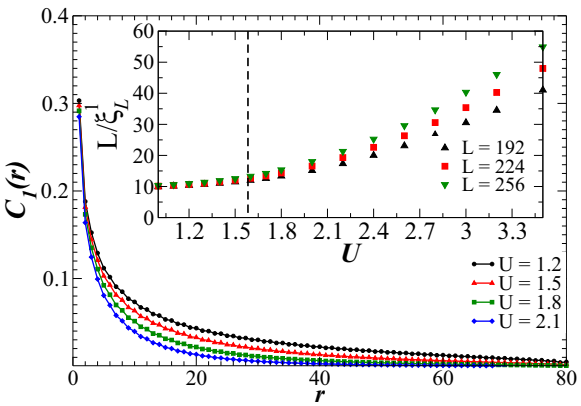

FIG. 6. (Color online) Plot of correlation function $C_1(r)$, as a function of r, at $V = 0.1$ and different values of U. In the inset, scaling of L/ξ^1_L as a function of U for $V = 0.1$. Coalescence of the data points of different system sizes shows SF-PSF transition at $U = 1.6 \pm 0.1$.

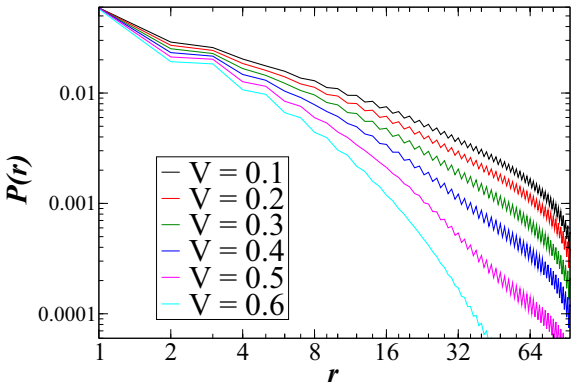

FIG. 7. (Color online) Plot of pair-correlation functions $P(r)$, as a function of r, on a log-log scale, at $U = 2.0$ and different values of V. The plot shows PSF to DW transition at $V = 0.4 \pm 0.05$.

undergoes transition from SF phase to PSF phase. In the inset of Fig. 6, we have plotted L/ξ_L^1 versus U. The coalescence of data occurs at $U = 1.6 \pm 0.1$ for different system sizes ($L = 192,224,256$). This indicates transition from SF to PSF phase at $U = 1.6 \pm 0.1$. We find, generically, SF to PSF transition to be the slowest transition in the phase diagram. The corresponding errors in finding the transition points have been indicated in the phase diagram.

C. PSF to DW transition

To characterize pair superfluidity, we have calculated the pair-correlation function, defined as $P(r) = \langle S^+_{1,0}S^+_{2,0}S^-_{1,r}S^-_{2,r}\rangle - \langle S^+_{1,0}S^-_{1,r}\rangle\langle S^+_{2,0}S^-_{2,r}\rangle$, where 1 and 2 stand for chain indices of the ladder and r is the distance from the middle site of the ladder. We find pair superfluidity in the system for lower values of repulsive interaction V and large enough values of attractive interaction U. With increase in V, we find density wave in each of the chains. We also find that, in the presence of large enough U, density wave in each of the chains gets stabilized at much lower values of V, and becomes strongly correlated [11]. In the PSF phase, correlation function, $P(r)$, decays algebraically, while, in the density wave phase, it decays exponentially. To reduce the finite-size effect, we have calculated $P(r)$ by taking the total system size $L = 384$ and with max value $m = 400$. In Fig. 7, we have plotted the pair-correlation function, $P(r)$, with r in log-log scale, at $U = 2$, and different values of V.

We find pair-correlation function, $P(r)$, and decay algebraically up to $V = 0.4 \pm 0.05$ for $U = 2.0$. For $V \geqslant 0.4 \pm 0.05$, the pair-correlation function decays exponentially, indicating transition from PSF to DW phase.

In Fig. 8, we have plotted correlation function, $G_1(r)$, as a function of r, at $U = 2.0$ and for different values of V. This shows how the density wave order develops in the chain with increase in repulsive interaction, V, while going from PSF to DW phase. In the inset of Fig. 8, we show extrapolation of $O_G(L)$ as a function of 1/L for different values of V, and for $U = 2.0$. From extrapolation of $O_G(L)$, it seems that for $V \gtrsim 0.3$, O_G takes a finite value for $U = 2$. As discussed in the SF to DW transition, from correlation function, $G_1(r)$, and finite-size scaling of O_G, we find that density wave order exists

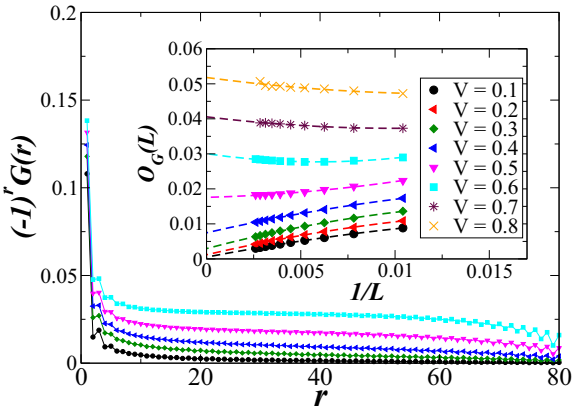

FIG. 8. (Color online) Plot of correlation function $(-1)^r G_1(r)$, as a function of r, at $U = 2.0$ and different values of V: $V = 0.1$ (circle), $V = 0.3$ (diamond), $V = 0.4$ (triangle left), $V = 0.5$ (triangle down), and $V = 0.6$ (square). Inset shows finite-size scaling of O_G, at $U = 2.0$ and different values of V.

in each of the chains for $V = 0.4 \pm 0.08$. As shown in Fig. 8 and the inset of Fig. 4, density wave order develops in each of the chains faster and stabilizes at much lower values of V, for $U = 2.0$ (Fig. 8) compared to $U = 0.5$ (Fig. 4). We find continuous transition from PSF phase to DW phase; we did not find PSS phase within our error bar.

D. Dimerization

With increase in attractive interaction, U, between the chains, bosons makes bound pairs along the rung, while, due to repulsive interaction V, these bound pairs try to avoid each other. As a result, in the large limit of U and V, positions of the hardcore bosons in each of the chains become strongly correlated. In this limit, the density waves of each of the chains are correlated to each other. To find this correlation in density waves of chains, we have calculated dimer-dimer correlation $D(r) = \langle S^z_{1,0}S^z_{2,0}S^z_{1,r}S^z_{2,r}\rangle$, where 1 and 2 stand for chain indices of the ladder and r is the distance from the middle site of the ladder. As shown in Fig. 9, we have plotted $D(r)$ with distance r for $V = 2.2$, and different values of U. For $U = 0$,

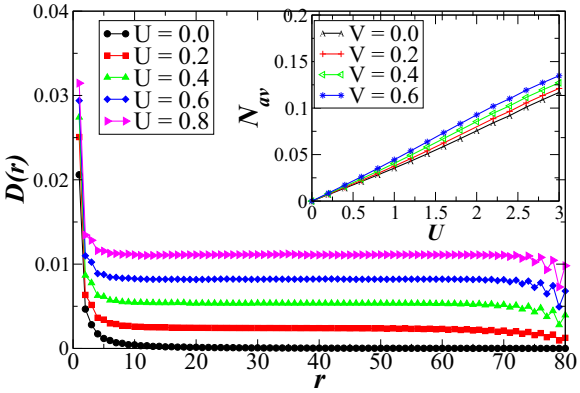

FIG. 9. (Color online) Plot of dimer-dimer correlation function $D(r)$, as function of r, for $V = 2.2$ and different values of U. Inset shows plot of N_{av} as a function of U, and different values of V.

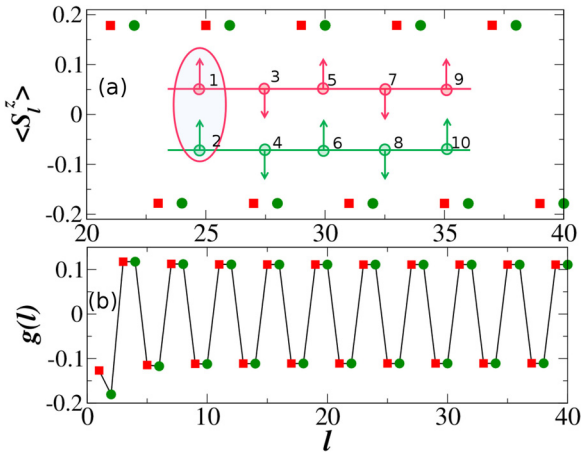

FIG. 10. (Color online) (a) Plot of spin density $\langle s_l^z \rangle$, as function of l, for $U = 2.0$ and $V = 1.5$. Spin density of the first chain is denoted with a square, while the second chain is denoted with a circle. Inset shows the schematic of dimerization of spins in two chains. (b) Plot of density correlation $g(l)$, as a function of l, for $U = 2.0$ and $V = 1.5$.

the two chains behave independently and, with increase in U, we find that the correlation in density wave increases. As already mentioned, increase in U forces bosons to make bound pairs along the rungs. The number of boson pairs in terms of spins can be defined as $N_{pair} = \sum_i \langle s^z_{1,i} s^z_{2,i} \rangle / \frac{L}{4}$, where i is the site index of the chain. For small values of U, since the system has large fluctuation effects, the number of pairs is quite small. In fact, in this limit, the system has loosely bound pairs along the rungs, while, with increase in U, N_{av} increases, displaying crossover of the system to strongly bound pairs. We also find that repulsive interaction, V, helps to stabilize these bound pairs. This is shown in the inset of Fig. 9, where we have plotted N_{av} versus U, for different values of V.

As we have discussed, in the large U and V limit, the system forms a density wave of strongly bound pairs and positions of hardcore bosons in each of the chains become strongly correlated [11,45]. In spin language, spins align ferromagnetically along the rung of the ladder, while antiferromagnetically along each of the chains [as shown in the schematic of Fig. 10(a)]. To show this, in Fig. 10(a), we have plotted spin density, $\langle S_l^z \rangle$, of the ladder with position l, for $U = 2$, and $V = 1.5$. For a clear view of $\langle S_l^z \rangle$, numbering of l index is done in a different way, which is shown in schematic of Fig. 10(a). Spin density, $\langle S_l^z \rangle$, along the rungs take same value and are in the same direction, while, along the chains, they are oriented in opposite directions. Such a configuration with parallel spin within each rung and antiparallel spin along each chain of the ladder structure can be represented as $|\uparrow\uparrow\downarrow\downarrow\uparrow\uparrow \ldots\rangle$. In hardcore bosonic language, due to attractive interaction, U, hardcore bosons form bound pairs along the rungs, while, due to repulsive interaction, V, present in each of the chains, these rung pairs try to avoid each other. As a result, these rung pairs reside on alternate rungs and this configuration can be represented by $|110011 \ldots\rangle$. As shown in Fig. 10(b), this configuration can also be visualized by looking at the density correlation function, $g(l) = \langle s_0^z s_l^z \rangle$, for both the chains (full ladder), where s_0^z is considered as the middle spin site of the ladder. Numbering of l index for $g(l)$, as shown schematically in Fig. 10(a), is done differently compared to $G_1(r)$. As shown in Fig. 10(b), periodicity of the density wave on the ladder is twice the lattice spacing. The structure factor, defined as $G(k) = \frac{1}{L/2} \sum_l \exp(ik \cdot l) \langle s_o^z s_l^z \rangle$, has peaks at $-\pi/2$ and $\pi/2$.

IV. CONCLUSION

In summary, we have studied various phases of hardcore bosons in two coupled chains, with interchain attraction and interchain nearest-neighbor repulsion between the bosons. We find that the ground state phase diagram has mainly three phases: SF, PSF, and DW. We have estimated the phases and the phase boundaries accurately through appropriate two body and four body correlation functions and at times the corresponding structure factors. The model discussed in this article is a simplified description of bilayer dipolar bosons with dipole moments perpendicular to the plane. Although we truncated the long range dipolar interaction to nearestneighbor repulsion, this model contains essential ingredients for the formation of "pair superfluid" and "pair density wave" phases. Similar to the BCS-BEC crossover of fermions, in this system, bosons can undergo a transition from a weakly bound paired superfluid state to density wave of strongly bound pairs.

ACKNOWLEDGMENTS

We would like to thank A. V. Mallik, Diptiman Sen, and Subroto Mukerjee for fruitful discussions. B.P. thanks the UGC, Govt. of India for support through a fellowship and S.K.P. acknowledges DST, Govt. of India for financial support.

[1] T. Lahaye, T. Koch, B. Fröhlich, M. Fattori, J. Metz, A. Griesmaier, S. Giovanazz, and T. Pfau, Nature (London) **448**, 672 (2007).
[2] M. Lu, N. Q. Burdick, S. H. Youn, and B. L. Lev, Phys. Rev. Lett. **107**, 190401 (2011).
[3] R. Löw, H. Weimer, J. Nipper, J. B. Balewski, B. Butscher, H. P. Büchler, and T. Pfau, J. Phys. B **45**, 113001 (2012).
[4] B. Yan, S. A. Moses, B. Gadway, J. P. Covey, K. R. A. Hazzard, A. M. Rey, D. S. Jin, and J. Ye, Nature (London) **501**, 521 (2013).
[5] M. Greiner, C. A. Regal, and D. S. Jin, Nature (London) **426**, 537 (2003).
[6] C. A. Regal, M. Greiner, and D. S. Jin, Phys. Rev. Lett. **92**, 040403 (2004).
[7] K.-K. Ni, S. Ospelkaus, M. H. G. de Miranda, A. Péer, B. Neyenhuis, J. J. Zirbe, S. Kotochigova, P. S. Julienne, D. S. Jin, and J. Ye, Science **322**, 231 (2008).
[8] A. Kuklov, N. Prokof'ev, and B. Svistunov, Phys. Rev. Lett. **92**, 050402 (2004).
[9] C. Chung, S. Fang, and P. Chen, Phys. Rev. B **85**, 214513 (2012).

[10] C. Trefzger, C. Menotti, and M. Lewenstein, Phys. Rev. Lett. **103**, 035304 (2009).
[11] A. Safavi-Naini, S. G. Söyler, G. Pupillo, H. R. Sadeghpour, and B. Capogrosso-Sansone, New J. Phys. **15**, 013036 (2013).
[12] A. Macia, G. E. Astrakharchik, F. Mazzanti, S. Giorgini, and J. Boronat, Phys. Rev. A **90**, 043623 (2014).
[13] J. Catani, L. De Sarlo, G. Barontini, F. Minardi, and M. Inguscio, Phys. Rev. A **77**, 011603(R) (2008).
[14] H. C. Jiang, L. Fu, and C. K. Xu, Phys. Rev. B **86**, 045129 (2012).
[15] E. Kim and M. H. W. Chan, Nature (London) **427**, 225 (2004).
[16] D. Y. Kim and M. H. W. Chan, Phys. Rev. Lett. **109**, 155301 (2012).
[17] D. L. Kovrizhin, G. V. Pai, and S. Sinha, Eur. Phys. Lett. **72**, 162 (2005).
[18] R. G. Melko, A. Paramekanti, A. A. Burkov, A. Vishwanath, D. N. Sheng, and L. Balents, Phys. Rev. Lett. **95**, 127207 (2005).
[19] P. Sengupta, L. P. Pryadko, F. Alet, M. Troyer, and G. Schmid, Phys. Rev. Lett. **94**, 207202 (2005).
[20] S. Sinha and L. Santos, Phys. Rev. Lett. **99**, 140406 (2007).
[21] H. C. Jiang, M. Q. Weng, Z. Y. Weng, D. N. Sheng, and L. Balents, Phys. Rev. B **79**, 020409(R) (2009).
[22] A. Bühler and H. P. Büchler, Phys. Rev. A **84**, 023607 (2011).
[23] N. Henkel, R. Nath, and T. Pohl, Phys. Rev. Lett. **104**, 195302 (2010).
[24] F. Cinti, P. Jain, M. Boninsegni, A. Micheli, P. Zoller, and G. Pupillo, Phys. Rev. Lett. **105**, 135301 (2010).
[25] X. Li, W. V. Liu, and C. Lin, Phys. Rev. A **83**, 021602(R) (2011).
[26] W. Zhang, R. Yin, and Y. Wang, Phys. Rev. B **88**, 174515 (2013).
[27] T. Giamarchi, *Quantum Physics in One Dimension* (Clarendon Press, Oxford, UK, 2004).
[28] T. D. Kühner and H. Monien, Phys. Rev. B **58**, R14741(R) (1998).
[29] T. D. Kühner, S. R. White, and H. Monien, Phys. Rev. B **61**, 12474 (2000).
[30] G. Roux, T. Barthel, I. P. McCulloch, C. Kollath, U. Schollwöck, and T. Giamarchi, Phys. Rev. A **78**, 023628 (2008).
[31] M. A. Cazalilla, R. Citro, E. Orignac, and M. Rigol, Rev. Mod. Phys. **83**, 1405 (2011).
[32] S. Ejima, F. Lange, H. Fehske, F. Gebhard, and K. zu Münster, Phys. Rev. A **88**, 063625 (2013).
[33] M. S. Luthra, T. Mishra, R. V. Pai, and B. P. Das, Phys. Rev. B **78**, 165104 (2008).
[34] A. Argüelles and L. Santos, Phys. Rev. A **75**, 053613 (2007).
[35] A. Hu, L. Mathey, I. Danshita, E. Tiesinga, C. J. Williams, and C. W. Clark, Phys. Rev. A **80**, 023619 (2009).
[36] L. Mathey, I. Danshita, and C. W. Clark, Phys. Rev. A **79**, 011602(R) (2009).
[37] L. Mazza, M. Rizzi, M. Lewenstein, and J. I. Cirac, Phys. Rev. A **82**, 043629 (2010).
[38] G. G. Batrouni, R. T. Scalettar, V. G. Rousseau, and B. Grémaud, Phys. Rev. Lett. **110**, 265303 (2013).
[39] A. Kundu and S. K. Pati, Eur. Phys. Lett. **85**, 43001 (2009).
[40] T. Mishra, R. V. Pai, S. Mukherjee, and A. Paramekanti, Phys. Rev. B **87**, 174504 (2013).
[41] T. Mishra, R. V. Pai, and S. Mukherjee, Phys. Rev. A **89**, 013615 (2014).
[42] T. Mishra, J. Carrasquilla, and M. Rigol, Phys. Rev. B **84**, 115135 (2011).
[43] G. Söyler, B. Capogrosso-Sansone, N. V. Prokof'ev, and B. V. Svistunov, New J. Phys. **11**, 073036 (2009).
[44] M. Guglielmino, V. Penna, and B. Capogrosso-Sansone, Phys. Rev. A **84**, 031603(R) (2011).
[45] A. Safavi-Naini, B. Capogrosso-Sansone, and A. Kuklov, Phys. Rev. A **90**, 043604 (2014).
[46] M. Singh, T. Mishra, R. V. Pai, and B. P. Das, Phys. Rev. A **90**, 013625 (2014).
[47] S. R. White, Phys. Rev. Lett. **69**, 2863 (1992); Phys. Rev. B **48**, 10345 (1993).
[48] U. Schollwöck, Rev. Mod. Phys. **77**, 259 (2005).
[49] R. V. Pai, R. Pandit, H. R. Krishnamurthy, and S. Ramasesha, Phys. Rev. Lett. **76**, 2937 (1996).
[50] R. V. Pai and R. Pandit, Phys. Rev. B **71**, 104508 (2005).
[51] G. G. Batrouni, R. T. Scalettar, G. T. Zimanyi, and A. P. Kampf, Phys. Rev. Lett. **74**, 2527 (1995).
[52] D. Rossini and R. Fazio, New J. Phys. **14**, 065012 (2012).
[53] J. M. Kosterlitz and D. J. Thouless, J. Phys. C **6**, 1181 (1973).